

## Synthesis and Protonation Behavior of Comblike Poly(ethyleneimine)

**Ger J. M. Koper***Laboratory of Physical Chemistry, Delft University of Technology, Julianalaan 136, 2628 BL Delft, The Netherlands***René C. van Duijvenbode and Danny D. P. W. Stam***Leiden Institute of Chemistry, Leiden University, PO Box 9502, 2300 RA, Leiden, The Netherlands***Ulrich Steuerle***BASF Aktiengesellschaft, 67056 Ludwigshafen, Germany***Michal Borkovec\****Department of Inorganic, Analytical, and Applied Chemistry, University of Geneva, 30 Quai Ernest-Ansermet, 1211 Geneva 4, Switzerland**Received May 28, 2002; Revised Manuscript Received February 4, 2003*

**ABSTRACT:** Comblike poly(ethyleneimine) (PEI) with  $-(CH_2CH_2)N(CH_2CH_2NH_2)-$  as the repeating unit has been synthesized by employing a protecting group strategy, and analyzed by potentiometric titration. If the degree of protonation is plotted as a function of pH, the titration curve shows three protonation steps separated by two intermediate plateaus, namely one at a degree of protonation of  $1/2$  and a second one at  $3/4$ . The first protonation step occurring at pH around 9.5 corresponds to the protonation of the primary amine groups on the side chains. During the second protonation step at pH around 4.5 every second tertiary amine protonates. The final protonation step, where the remaining tertiary amines protonate, is suspected to occur in a pH range near 0. The latter point and the detailed protonation mechanism are deduced on the basis of a site-binding model. The model, which has been independently calibrated on titration data of low molecular weight amines, is capable to predict the titration curve quantitatively to a good degree of accuracy.

**Introduction**

Recently, one could witness substantial progress in the understanding of the protonation behavior of weak polyelectrolytes.<sup>1–14</sup> These studies have reached two relevant conclusions, which have been hardly appreciated in the past. First, the interactions operating between ionizable sites are short ranged, and can be effectively approximated by nearest neighbor interactions.<sup>2</sup> Second, the protonation behavior of branched polyelectrolytes differs substantially from that of their linear analogues.<sup>3,4</sup>

Interactions between ionizable groups are dominated by electrostatic forces. Such forces are known to be long-ranged, and the short-range character of site–site interactions may seem surprising. It must be noted, however, that these interactions are very strong at short distances, as they are mediated by the polyelectrolyte backbone of low dielectric permittivity. At larger distances, they are weakened by the high-permittivity of water and the screening by salt. Within the crossover between the interactions dominated by the low-permittivity medium (strong interactions) and the high-permittivity medium (weaker interactions), the interactions decay very quickly, and only neighbors within the immediate vicinity are of relevance. One should note, however, that the problem is subtle as the geometry of the dielectric medium enters. The scenario of short-ranged interactions is only applicable to polyelectrolytes. In the case of interfaces, for example, the interactions are long ranged, as one would expect

intuitively. In the case of long-range interactions, correlations between the sites are weak, mean-field approximation is usually excellent, and one typically obtains broad and featureless titration curves. On the other hand, correlations are more important for polyelectrolytes, where interactions are short-ranged, titration curves show more structure, and cannot be explained with mean-field models. More details on these aspects can be found in the literature.<sup>1,2,15</sup>

The second conclusion concerning the differences between the protonation patterns between linear and branched polyelectrolytes represents an immediate consequence of the short-ranged nature of the site–site interaction potential. Once these interactions are known, the expected protonation pattern follows from a discrete site-binding model.<sup>1,3,4,6</sup> Within this model, which is analogous to the Ising model known from statistical mechanics, the protonation state of each ionizable site is characterized by a discrete two valued state variable (i.e., protonated and deprotonated). On the basis of this model, the protonation pattern can be deduced using standard statistical-mechanical methods. This approach will also be used in this paper to interpret the protonation of comblike poly(ethyleneimine) (PEI).

While we shall discuss the site-binding model and its analysis in its full detail later, at this point it is appropriate to review some theoretically expected differences between the protonation patterns of linear and branched polyelectrolytes.<sup>3,4</sup> In the simplest nontrivial situation one may consider all ionizable sites being equivalent, and having the same affinity to protons. One can further assume that all site–site interactions can

\* Corresponding author.

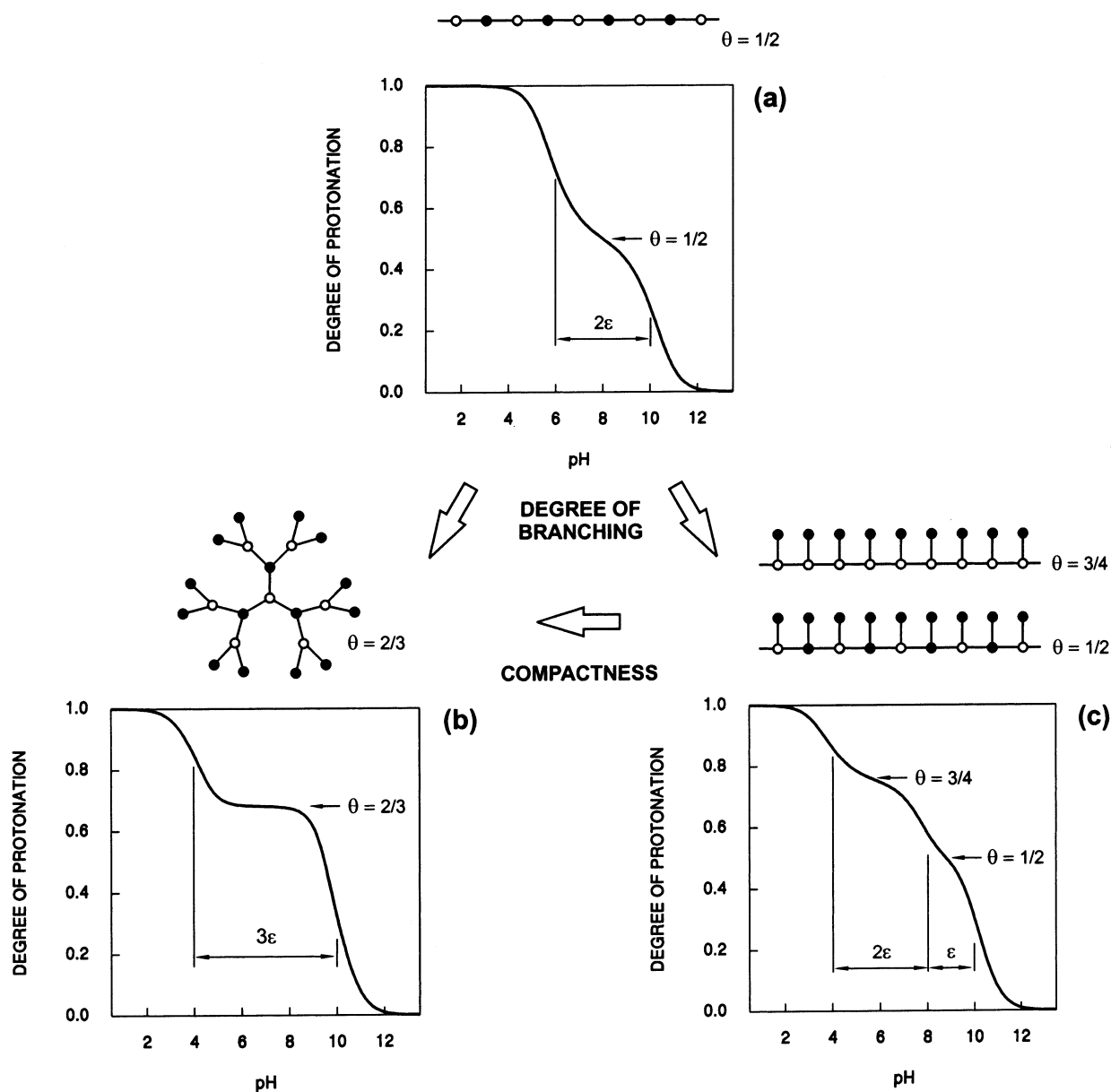


**Figure 1.** Schematic representation of the influence of compactness and degree of branching on the protonation of poly(ethyleneimine) (PEI). All titration curves were calculated by assuming all sites to be equivalent with a ionization constant of  $pK = 10$  and a nearest neighbor pair interaction parameter  $\epsilon = 2$ . Horizontal arrows denote the degree of protonation of the apparent plateaus, while horizontal lines demote the splitting between the apparent protonation steps. The intermediate plateaus correspond to the protonation states shown above. The amine groups are indicated by circles and the connecting ethylene chain is indicated by a line. Closed and open circles symbolize protonated and deprotonated amines, respectively. (a) Linear chain, (b) dendrimer, and (c) comb.

be approximated with nearest neighbor interactions, thereby neglecting all higher order interactions. This model has merely two parameters, a microscopic ionization constant denoted as  $pK$  and a pair interaction parameter  $\epsilon$ . The  $pK$  value characterizes the affinity of protons toward the ionizable sites in the absence of interactions, while the pair interaction parameter  $\epsilon$  is the free pair interaction energy in thermal units (and further includes an unimportant numerical factor). It was argued elsewhere that this simple model captures most features of the protonation of real polyelectrolytes astonishingly well. In particular, it can be used to interpret the protonation behavior of poly(ethyleneimines) (PEI) with  $[-N-CH_2-CH_2-]_n$  as the repeating unit.<sup>4,6</sup>

Figure 1 contrasts the predicted titration curves (i.e., degree of protonation  $\theta$  as a function of pH) for linear and branched polyelectrolytes. Figure 1a recapitulates

the classical case of the linear chain. The titration curves shows two distinct protonation steps, and an intermediate plateau at  $\theta = 1/2$ . This characteristic shape can be understood as follows. At high pH, the majority of the sites are deprotonated. Therefore, the protons begin to bind to the chain independently, leading to an apparent protonation step near  $pH \approx pK = 10$ . With decreasing pH, additional sites will protonate, until one reaches  $\theta = 1/2$ . At this point, the chain tends to minimize its free energy by protonating every second site, as this intermediate configuration avoids all nearest neighbor pair interactions. When the pH is lowered further, the chain will eventually protonate fully. However, in the intermediate configuration every unprotonated site has two protonated neighbors, and further protonation can only occur by overcoming two pair interactions, namely at  $pH \approx pK - 2\epsilon = 6$ . The

two separate protonation steps can be seen clearly in titration curves of various highly charged linear polyelectrolytes, such as PEI, poly(vinylamine), or poly(maleid acid).<sup>1,6,8,9</sup> More weakly charged polyelectrolytes, such as poly(acrylic acid) or hyaluronic acid, titrate in a single protonation step, since the interactions are not sufficiently strong to induce the two-step behavior.<sup>1,8</sup>

Analogous reasoning can be applied to branched polyelectrolytes. However, one faces two complications. First, a branched structure contains sites with different numbers of nearest neighbors, and in practice groups with one, two, and three nearest neighbor sites may occur. On the other hand, the infinite linear chain features sites with two nearest neighbors only. In the case of PEI, the linear structure contains only secondary amines, while for branched systems, primary, secondary, and tertiary amine groups might be present. Second, a great variety of branched structures exist even within this simple model, but only one type of linear chain exists. One must therefore introduce some systematic classification of branched polymers.

One possible classification of branched polyelectrolytes was discussed recently.<sup>3</sup> In many practical situations, one can approximate the relevant structures by trees. Within this simplification one assumes no closed loops within the structure. Many types of branched polyelectrolytes fall into this class. In this case, the branched structure can be characterized with two parameters, namely *degree of branching* and *compactness*. Let us illustrate these structural parameters for the case of PEI. The degree of branching is familiar to most polymer chemists; this parameter decreases with increasing fraction of secondary amine groups. The linear chain contains only secondary amine groups and corresponds to the least branched structure, while a highly branched structure contains a large fraction of tertiary amine groups. The *compactness* is determined by the coordination of the tertiary amine groups. The larger the fraction of tertiary amine groups that are directly connected to primary amines, possibly through secondary amines, the smaller is the degree of compactness. The most compact structure is the dendrimer (see Figure 1b),<sup>16,17</sup> while the least compact structure is the comb (see Figure 1c).

The dendrimer and the comb represent the extremes among the branched structures; all other structures can be thought as intermediates between those and the linear chain. For this reason, it is important to understand the protonation behavior of the dendrimer and the comb. Results from the simple site-binding model are most illustrative. Since the protonation of the dendrimer is somewhat simpler, it will be discussed first. The protonation of the comb will be discussed thereafter.

Figure 1b illustrates the protonation behavior of a dendrimer. The situation is qualitatively similar to the linear polyelectrolyte discussed initially. The titration curve again shows two distinct protonation steps, and one intermediate plateau. However, the plateau now occurs at  $\theta = 2/3$ . This characteristic shape can be understood similarly as for the linear polyelectrolyte. At high pH, the protons bind to the dendrimer independently, leading to a protonation step near  $\text{pH} \approx \text{p}K = 10$ . With decreasing pH, additional sites will protonate, until one reaches  $\theta = 2/3$ . At this point, the dendrimer can minimize its free energy by avoiding all nearest neighbor pair interactions by protonating every odd shell in an onionlike pattern (see Figure 1b). At even

lower pH, the dendrimer will protonate fully, but since in the intermediate state every unprotonated site is neighbored by three protonated sites, the second step occurs at  $\text{pH} \approx \text{p}K - 3\epsilon = 4$ .

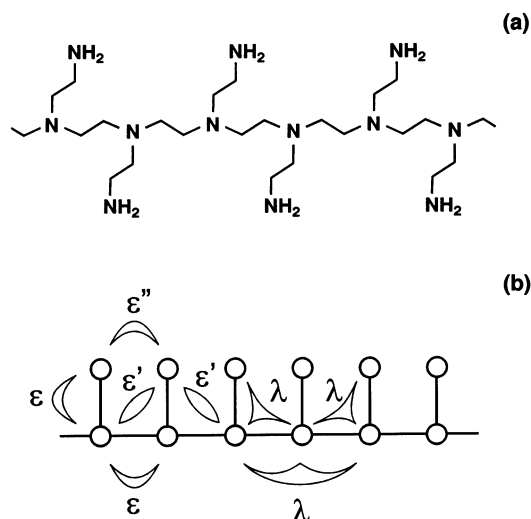
This protonation pattern has been recently confirmed experimentally by studying the protonation of various generations of poly(propyleneimine) dendrimers by means of potentiometric titrations<sup>18</sup> and <sup>15</sup>N NMR.<sup>19</sup> In particular, the latter technique provides information on the individual sites, and one can unequivocally show that in the intermediate state only the odd shells are protonated.

Figure 1c summarizes the predictions of this site-binding model for the comb. The titration curve now displays three protonation steps and two intermediate plateaus, one at  $\theta = 1/2$ , and the other at  $\theta = 3/4$ . This structure can be understood similarly as before. At high pH, the protons bind to the comb independently, leading to a protonation step near  $\text{pH} \approx \text{p}K = 10$ . With decreasing pH, additional sites will protonate, until one reaches  $\theta = 1/2$ . At this point, the comb can minimize its free energy by avoiding all nearest neighbor pair interactions by adopting an intermediate configuration where all side groups (primary amines) are protonated, and the groups along the backbone unprotonated (tertiary amines; see Figure 1c). If the pH is lowered further, the comb will protonate additional sites, but since in the intermediate configuration every unprotonated site is neighbored by one protonated site, the second step occurs at  $\text{pH} \approx \text{p}K - \epsilon = 8$ . Lowering the pH further, the comb will protonate until one reaches  $\theta = 3/4$ . At this point, the comb can again minimize its free energy, but only with a second intermediate configuration invoking one nearest neighbor pair interaction for every two sites. This intermediate configuration has all side groups (primary amines) and every second group along the backbone protonated (tertiary amines, see Figure 1c). When the pH is lowered even further, the comb will fully protonate, but since in the second intermediate configuration every unprotonated site is neighbored by three protonated sites, the second step occurs at  $\text{pH} \approx \text{p}K - 3\epsilon = 4$ .

These results for the comb were so far entirely hypothetical, as the protonation behavior of such polyelectrolytes has never been studied. The present article focuses on comb-PEI (see Figure 2), where the backbone consists of tertiary amine groups and the side chain of a single primary amine group. We compare experimental titration data with calculations based on a site-binding model. Since comb-PEI is not available commercially, we have developed a synthetic route, which is described here in detail. We find that the results of potentiometric titrations are in full agreement with the site-binding model, and provide a further support for its validity.

### Site-Binding Model for Linear and Comblike Polyelectrolytes

Protonation equilibria in polyprotic systems can be described with a site-binding model, which is equivalent to the Ising model known in the statistical mechanics literature.<sup>1,3,4,6,10–12</sup> Ionizable sites are labeled by an index  $i = 1, 2, \dots, N$  where  $N$  is the total number of sites. The protonation state of each site  $i$  is characterized by a two-value state variable  $s_i$ , which is defined such that  $s_i = 0$  if the site is deprotonated and  $s_i = 1$  if the site is protonated. The protonation state of the entire molecule



**Figure 2.** Definitions of model parameters for comb-PEI: (a) structural formula, and (b) definition of the various interaction parameters used to predict the titration behavior. Nearest neighbor pair and triplet interaction parameters are denoted by  $\epsilon$  and  $\lambda$ , respectively. Next nearest neighbor pair interaction parameter between tertiary and primary amine groups is given by  $\epsilon'$  (see Table 1). The model assumes the ionization constants  $pK^{(1)}$  and  $pK^{(3)}$  to be different, and introduces three types of interactions.<sup>3,4</sup> The strongest are nearest neighbor pair interactions between amine groups characterized with the parameter  $\epsilon$ . These are assumed to be equal for tertiary-tertiary and primary-tertiary interactions. Nearest neighbor triplet interactions between amine groups are described with the parameter  $\lambda$ , and again they are assumed to be the same for all different possible triplets. Finally, next nearest neighbor pair interaction acts between two tertiary amine groups along the backbone and one primary amine group on the side chain, and are parametrized by  $\epsilon'$ . The analogous interactions along the backbone are negligible.<sup>7</sup>

(i.e., its microstate) is fully determined by the set of the state variables  $s_1, s_2, \dots, s_N$ . The free energy of a given microstate, where the conformational and other degrees of freedom have been preaveraged, can be expressed in terms of an expansion in terms of these site variables as<sup>1,11,12</sup>

$$\frac{\beta F(s_1, s_2, \dots, s_N)}{\ln 10} = \sum_i (pH - pK_i) s_i + \sum_{i < j} \epsilon_{ij} s_i s_j + \sum_{i < j < k} \lambda_{ijk} s_i s_j s_k + \dots \quad (1)$$

where  $1/\beta = kT$  denotes the thermal energy, pH is the negative common logarithm of the proton activity,  $pK_i$  is the negative common logarithm of the microscopic dissociation constant of site  $i$  given all other groups are being deprotonated,  $\epsilon_{ij} > 0$  characterizes the strength of the pair interactions between sites  $i$  and  $j$ , and  $\lambda_{ijk}$  of the triplet interactions involving sites  $i, j$ , and  $k$ . As discussed in the Introduction, the pair (and triplet) interactions are short ranged, and only nearest or next nearest neighbor ones have to be taken into account. Any higher order interactions will be neglected.

All system properties can be obtained from the partition function

$$\Xi = \sum_{\{s_1, s_2, \dots, s_N\}} e^{-\beta F(s_1, s_2, \dots, s_N)} \quad (2)$$

and the titration curve, which represents the average degree of protonation  $\theta$  as a function of pH, is given by

$$\theta = \frac{a_H}{N} \frac{\partial(\ln \Xi)}{\partial a_H} \quad (3)$$

where  $a_H$  is the activity of the protons, i.e.,  $pH = -^{10}\log a_H$ .

The partition function can be exactly evaluated for linear structures and short ranged interactions with the transfer matrix technique.<sup>3,20</sup> The partition function can be expressed in terms of a suitably chosen transfer matrix, which is defined such that the partition function can be obtained by evaluating products of this matrix. In the limit of a large number of sites, the partition function can be shown to be proportional to<sup>20</sup>

$$\Xi \propto \lambda^N \quad (4)$$

where  $\lambda$  is the largest eigenvalue of the transfer matrix, and the proportionality constant becomes unimportant for  $N \gg 1$ . This technique makes the evaluation of the partition function of arbitrary polyelectrolytes straightforward, as one only has to calculate the largest eigenvalue of the transfer matrix.

The transfer matrix for a linear chain with nearest neighbor interactions has dimensions  $2 \times 2$  as has been discussed repeatedly.<sup>1,3</sup> The matrix describes the propagation step from one site to the next along the chain, and reads

$$\begin{pmatrix} 1 & z \\ 1 & zu \end{pmatrix} \quad (5)$$

where the strength of the pair interactions is expressed in terms of  $\epsilon = -^{10}\log u$  and  $^{10}\log z = pK - pH$  where  $pK$  is the ionization constant of the group. The largest eigenvalue can be evaluated analytically, and with eq 3, one can obtain an analytical expression for the titration curve of a linear polyelectrolyte with nearest neighbor interactions. The result was discussed in the Introduction and is plotted in Figure 1a.

Nearest neighbor triplet interactions can be incorporated by considering steps from a pair of successive sites to the next pair along the chain. The dimensions of the transfer matrix are now  $4 \times 4$  and the matrix reads<sup>5</sup>

$$\begin{pmatrix} 1 & z & z & z^2 u \\ 1 & z & zu & z^2 u^2 w \\ 1 & z & z & z^2 u \\ 1 & z & zuw & (zuw)^2 \end{pmatrix} \quad (6)$$

where the triplet interactions are parametrized by  $\lambda = -^{10}\log w$ . The partition function can be again calculated from the largest eigenvalue of the transfer matrix.

Consider now the comb with side chains involving just a single additional site (see Figure 2). Considering nearest neighbor pair interactions only, the transfer matrix steps again from site to site along the chain. However, each step involves two sites, namely one on the side chain and the second on the backbone. The corresponding matrix reads

$$\begin{pmatrix} 1 & z_1 & z_3 & z_1 z_3 u \\ 1 & z_1 & z_3 v & z_1 z_3 uv \\ 1 & z_1 v & z_3 u & z_1 z_3 u^2 v \\ 1 & z_1 v & z_3 vu & z_1 z_3 u^2 v^2 \end{pmatrix} \quad (7)$$



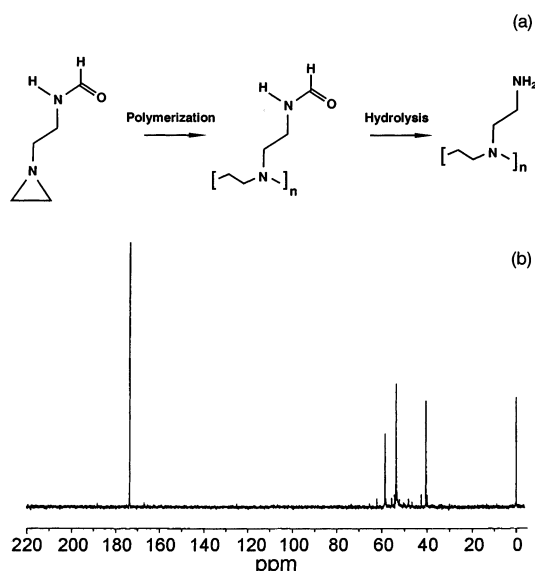


**Figure 3.** Synthesis and characterization the comb-PEI: (a) polymerization of *N*-(2-(1'-aziridino)ethyl)formamide and subsequent hydrolysis, and (b)  $^{13}\text{C}$  NMR spectrum in  $\text{D}_2\text{O}$  of the final product prior to membrane filtration.

where  $^{10}\log z_1 = p\hat{K}^{(1)} - \text{pH}$  and  $^{10}\log z_3 = p\hat{K}^{(3)} - \text{pH}$ . The ionization constants of the primary groups on the side chain and of the tertiary groups at the backbone are denoted by  $p\hat{K}^{(1)}$  and  $p\hat{K}^{(3)}$ . Next nearest neighbor pair interactions along the side chains are parametrized with  $\epsilon' = -^{10}\log v$  (cf. Figure 2b). The analogous interactions along the backbone are neglected. The result shown in Figure 1c has been obtained by setting  $\epsilon' = 0$  and  $p\hat{K}^{(1)} = p\hat{K}^{(3)}$ .

The transfer matrix that also includes the triplet interactions involves four sites for each step, namely two along the backbone and the corresponding side chains. This  $16 \times 16$  matrix is too involved to reproduce. Those interested can obtain an electronic text file with a listing of the matrix elements from the corresponding author.

One should realize that the number  $N$  entering eq 4 must be modified accordingly. For eq 6 the number of sites is given by  $N$ , as the matrix steps only by one, while for eq 7  $N$  corresponds to half the number of sites. Analogous considerations apply to the  $16 \times 16$  matrix involving triplet interactions.

## Materials and Experimental Methods

**Synthesis.** Comblike PEI has been synthesized by employing a protecting group strategy. The scheme of the reaction is shown in Figure 3a. In this approach, one polymerizes *N*-(2-(1'-aziridino)ethyl)formamide<sup>21</sup> first, and the resulting linear polymer is subsequently hydrolyzed.

*N*-(2-(1'-Aziridino)ethyl)formamide was polymerized in the presence of sulfuric acid in water. To a solution of 57 g of water and 0.5 g of sulfuric acid (0.005 mol) at 50 °C, one adds 57 g of *N*-(2-(1'-aziridino)ethyl)formamide (0.5 mol) within 20 min. The solution was stirred for 70 h. The degree of hydrolysis of the resulting poly(*N*-(2-(1'-aziridino)ethyl)formamide), as determined by  $^1\text{H}$  NMR, was about 5%. The hydrolysis of the product was achieved in alkaline conditions. To a solution of 37.5 g of poly(*N*-(2-(1'-aziridino)ethyl)formamide) (0.33 mol) in 112.5 g of water was added 26.4 g of a 50% NaOH solution (0.33 mol). The solution was stirred at 95 °C for 5 h.

The structure of the resulting comblike PEI was confirmed by NMR. The chemical shifts from  $^1\text{H}$  NMR in  $\text{D}_2\text{O}$  are  $\delta = 2.6\text{--}2.8$  (8 H, m), 8.5 (1 H, s, sodium formate). The  $^{13}\text{C}$  NMR spectrum in  $\text{D}_2\text{O}$  is shown in Figure 3b; the chemical shifts are  $\delta = 40.5$  ( $\text{CH}_2$ ), 53.7 ( $\text{CH}_2$ ), 58.6 ( $\text{CH}_2$ ), 173.6 (CH, sodium

formate). On the basis of the known patterns of  $^{13}\text{C}$  NMR spectra of aliphatic polyamines,<sup>22,23</sup> the spectrum showing three  $\text{CH}_2$ -resonances confirms the comblike structure. The  $\delta = 40.5$  resonance is characteristic for a  $\text{CH}_2$  group next to a primary amine group, while the other two resonances with  $\delta > 53$  correspond to  $\text{CH}_2$  groups next to tertiary amine groups. Signals from  $\text{CH}_2$  groups next to secondary amine groups, which would be expected around 47–50, are missing in the present molecule. These findings are in contrast to linear PEI,<sup>24</sup> which shows a single line spectrum at  $\delta = 49.5$ , and to randomly branched PEI, which shows an eight-line  $^{13}\text{C}$  NMR spectrum.<sup>25,26</sup> Another indication for the proposed structure is the  $^{13}\text{C}$  NMR spectrum of the intermediate product, poly(*N*-(2-(1'-aziridino)ethyl)formamide), which did show, besides the quite similar  $\text{CH}_2$  three-line spectrum, an additional doublet near  $\delta = 161.0$  and 164.7. This resonance hybrid is characteristic for the formamido-group terminating the side branch.

The degree of polymerization of the comb-PEI was about 158. It was estimated from the molecular mass of the non-hydrolyzed polymer (approximately 18 kDa) obtained by static light scattering and differential refractometry. For the potentiometric titrations, sodium formate and oligomeric impurities were removed by means of membrane filtration. The oligomeric impurities were identified by GC-MS to consist mainly of dimers and were found to be below 7% by gel permeation chromatography.

**Potentiometric Titrations.** The degree of protonation was determined with a commercial, high precision computer-controlled titration instrument,<sup>27</sup> which utilizes a separate glass electrode and an Ag/AgCl reference electrode with a salt bridge. Four burets were used for acid solution, base solution, brine, and pure water, a procedure which allows us to keep a constant ionic strength during the titration experiments. Details are given elsewhere.<sup>19,28</sup> The degree of protonation as a function of pH is obtained by subtracting the titration curve of the sample from a blank titration curve of a pure electrolyte solution at the same ionic strength. The total nitrogen content of the samples, as determined by elemental nitrogen analysis, is used to normalize the curves to the degree of protonation. The accuracy of this method is, in the pH range from 3 to 11, estimated at  $\pm 0.05$  on the pH scale and  $\pm 0.02$  in the degree of protonation.

## Results and Discussion

Figure 4 compares the experimental titration data of the comb-PEI at an ionic strength of 1 M with model predictions of the site-binding model.

Qualitatively, the shape of the experimental titration curve is consistent with the simplified discussion presented in the Introduction. One observes two intermediate plateaus, namely one at  $\theta = 1/2$  and the other at  $\theta = 3/4$ . While three protonation steps are expected, only two are apparent in the data. The first step occurs at pH near 9.0–9.5 and the second around 4.5–5.0. The last protonation step, which would be expected at low pH around 0, lies outside of the experimentally accessible pH window.

Let us now compare the data with the site-binding model discussed above. The parameters were defined in Figure 2b. The model assumes the ionization constants  $p\hat{K}^{(1)}$  and  $p\hat{K}^{(3)}$  to be different, and introduces three types of interactions.<sup>3,4</sup> The strongest are nearest neighbor pair interactions between amine groups characterized with the parameter  $\epsilon$ . On the basis of the available data, they are assumed to be equal for tertiary–tertiary and primary–tertiary interactions. Nearest neighbor triplet interactions between amine groups are described with the parameter  $\lambda$ , and again they are assumed to be the same for all different possible triplets. Finally, next nearest neighbor pair

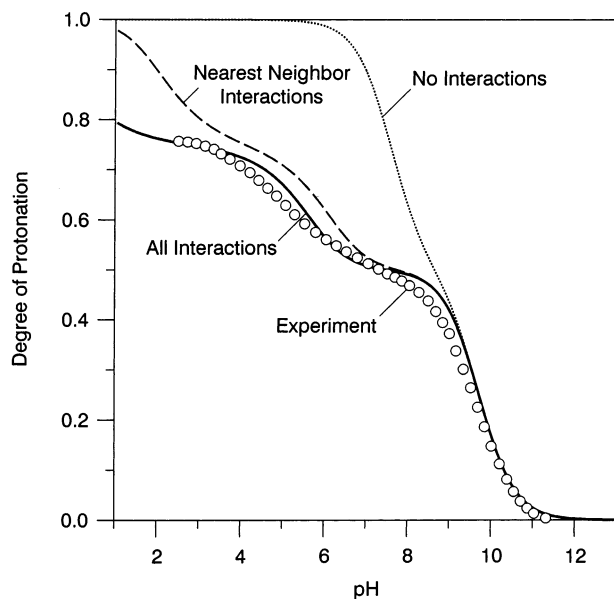


**Figure 4.** Potentiometric titration curves for comb-PEI at an ionic strength of 1 M. Symbols represent measured data and lines are the results of calculations based on the site-binding model. Full line is the calculation including all interactions. The dashed line includes nearest neighbor interactions only, while the dotted line is the result without interactions. Parameter values are taken from Table 1.

**Table 1. Parameters of the Site Binding Used for the Prediction of the Titration Curves for Different Ionic Strengths**

parameter <sup>a</sup>	0.1 M	0.5 M	1.0 M
$pK^{(1)}$	9.42	9.64	9.72
$pK^{(3)}$	7.20	7.50	7.60
$\epsilon$	1.97	1.85	1.75
$\epsilon'$	0.31	0.27	0.25
$\lambda$	0.42	0.42	0.42

<sup>a</sup> See Figure 2 for a graphical explanation. The parameters are obtained from an extensive analysis of small molecules.<sup>3,4,7</sup>

interaction act between two tertiary amine groups along the backbone and one primary amine group on the side chain, and are parametrized by  $\epsilon'$ . The analogous interactions along the backbone are negligible.<sup>7</sup>

A consistent set of these parameters for aliphatic polyamines was derived recently.<sup>3,4,7</sup> Their values are ionic strength dependent and are summarized in Table 1. These parameters were all estimated from ionization constants of different low-molecular weight amines. The procedure was to use the site-binding model for the evaluation of the macroscopic proton binding constants of various oligomeric PEI analogues. By comparing these predictions with the available experimental database of binding constants, these parameters can be extracted. It has been shown that this model can reliably predict proton binding constants of linear oligoamines at ionic strengths between 0.1 and 1 M, and of various branched oligoamines at 0.5 M. We have extended the latter analysis for PEI to the ionic strengths 0.1 and 1 M. The corresponding parameters are summarized in Table 1. It is essential to realize that no reference to any titration data of polymeric amines has been made in estimating them.

Figure 4 shows two different predictions of this model for the comb-PEI based on the transfer matrix technique using the parameters in Table 1. The solid line is the result of the calculation including all interactions.

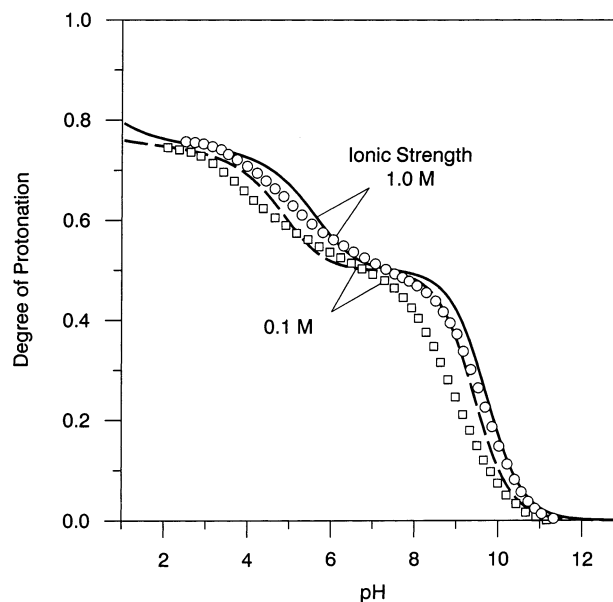


**Figure 5.** Potentiometric titration curves for comb-PEI at ionic strength of 0.1 and 1 M. Symbols represent measured data and lines are the results of calculations based on the site-binding model including all interactions. Parameter values are taken from Table 1.

For comparison, the dashed line shows the corresponding result with nearest neighbor pair interactions only (i.e.,  $\epsilon' = \lambda = 0$ ), while the dotted line the result without any interactions (i.e., with  $\epsilon = \epsilon' = \lambda = 0$ ).

The simplified nearest neighbor pair interaction model reproduces all important features of the curve, but at low pH it predicts the comb to be more basic than it actually is. This curve differs somewhat from the simplified picture presented in the Introduction (Figure 1c) due to the larger acidity of the tertiary amine group with respect to the primary one. The first protonation step is given due to the protonation of the primary amine groups at the side chain, and occurs at  $pH \approx pK^{(1)} = 9.72$ . The second protonation step involves every second tertiary amine groups, and in addition one pair interaction must be overcome, since the primary groups are already protonated. This step is therefore located at  $pH \approx pK^{(3)} - \epsilon = 5.85$ . The last protonation step is due to the protonation of the remaining tertiary amine groups, and involves three pair interactions. It occurs at  $pH \approx pK^{(3)} - 3\epsilon = 2.35$ . This scheme corresponds precisely to the protonation mechanism shown in Figure 1c. One observes that interactions are essential to explain the intermediate plateau at  $\theta = 3/4$ . A model without interactions predicts only two steps in the titration curve (see Figure 4).

The complete model involving all interactions shifts the calculated curve into the acidic region. Given the facts that no parameter adjustment has been made and that all parameters were determined independently, the agreement must be considered as very good. The main improvement over the simplified model is in the prediction of the correct location of the second protonation step, which is now shifted to lower pH. The triplet interaction parameter  $\lambda$  turns out to be unimportant. It only comes into play at the lowest pH values, and in the experimentally accessible region causes a widening of the plateau at  $\theta = 3/4$ .

Figure 5 compares the experimental data at 0.1 and 1.0 M, and we also include the predictions of the site-binding model with parameters from Table 1. As is

typical for a polybase, the titration curve shifts to lower pH with decreasing ionic strength. The quality of the model prediction is inferior at 0.1 M, but still rather satisfactory given the fact that the model was calibrated completely independently.

The reasons for the obvious discrepancies between experiment and model predictions are difficult to pinpoint at this stage. They could originate from experimental artifacts as well as from an inadequate parametrization of the model. On the experimental side, we suspect defects in the polymer structure as well as presence of oligomeric impurities, both probably in the range of 5–10%. In the former case, the incomplete hydrolysis increases the relative amount of tertiary amine groups and probably causes a small shift of the titration curve to lower pH. Incomplete hydrolysis, which is estimated around 5%, might well be the reason for the discrepancy between model and experiment at higher pH. The effect of oligomers may lead to shifts of the curve as well. Since the employed site-binding model has now been verified with such a wide variety of PEI analogues, the conceptual framework is surely appropriate. Nevertheless, it is conceivable that present parametrization of the more distant interactions within the branched structures is inaccurate. Only a limited number of branched PEI oligomers have been studied so far, and for this reason it is conceivable that the parameters proposed in Table 1 may require revision. For example, the agreement between model and experiment for the first protonation step can be made almost perfect by introducing a small pair interaction parameter (ca. 0.2–0.5) between the adjacent primary amine groups. Another possibility for the discrepancy could be related to the unusually high charge density of the comb-PEI chain. The importance of long-range electrostatic interactions, which are not included in the present model, would lead to a broadening of the calculated curves. Such interactions could be included on a mean-field basis and would probably bring the curves in better agreement with experiment. On the other hand, strong nearest-neighbor interactions are essential to describe the structure of the observed titration curve. Any mean-field model, which does not include such interactions explicitly, will fail to describe the observed titration curve.

## Conclusions

Comblike poly(ethyleneimine) (PEI) protonates in three steps. The primary groups on the side chains protonate first at pH around 9.0–9.5, which leads to a first intermediate plateau in the degree of protonation at  $\theta = 1/2$ . The second protonation occurs at pH near 4.5–5.0, and results in a second intermediate plateau at  $\theta = 3/4$ . At the second intermediate plateau all primary groups, but only every second tertiary amine group is protonated in an alternating fashion. The remaining tertiary groups protonate in a last protonation step at very low pH. This protonation step has not been observed in the present work, and lies probably in the pH range of  $-1.0$  and  $+0.5$ .

The two-step protonation behavior of the tertiary groups may seem surprising at first, but it is caused by the strong site-site interactions between the tertiary groups acting along the backbone. A similar behavior is well-known from strongly charged linear polyelectrolytes, which also protonate in two steps.<sup>1,2</sup> It is also essential to properly relate the first protonation step

between  $\theta = 1/2$  and  $3/4$  to the ionization constant of the tertiary amine group. This protonation step does correspond to the ionization constant of the tertiary group, but this is a microscopic constant of the tertiary group given that the neighboring primary amine group is protonated and the tertiary one is deprotonated. On the other hand, the microscopic ionization constant of an tertiary amine group in PEI, given the neighboring groups are deprotonated, lies near  $pK \approx 7.5$ . Protonation of a neighboring primary amine groups lowers its value by approximately 2 pH units. The protonation of the other two neighboring tertiary groups further lowers its value by about four more pH units. The latter corresponds to the last protonation step, which lies outside the accessible pH window.

The corresponding titration curve can be predicted to reasonable accuracy from an independently calibrated site-binding model. While the agreement between prediction and experiment is not perfect, the model predicts all relevant features observed experimentally. The success of this model can be therefore considered as a confirmation of the proposed protonation mechanism of the comblike PEI. The essential ingredient to the site-binding model is the proper consideration of nearest-neighbor interactions between the groups on the backbone. Models of the titration curves will fail qualitatively, they neglect interactions between the groups, or they only include them on a mean-field level only.

**Acknowledgment.** The authors would like to thank Anton Rajanayagam and Jacques van der Ploeg for their help in obtaining the titration curves, Gerhard Krack for the NMR measurements, and Horst Schuch for the molecular weight determination. Partial financial support was provided by the Swiss National Science Foundation.

## References and Notes

- (1) Borkovec, M.; Jönsson, B.; Koper, G. J. M. In *Surface and Colloid Science*; Matijević, E., Ed.; Kluwer Academic/Plenum Press: New York, 2001; Vol. 16, pp 99–339.
- (2) Borkovec, M.; Daicic, J.; Koper, G. J. M. *Proc. Natl. Acad. Sci. U.S.A.* **1997**, *94* 3499–3503. Borkovec, M.; Daicic, J.; Koper, G. J. M. *Physica A* **2001**, *298*, 1–23.
- (3) Borkovec, M.; Koper, G. J. M. *Macromolecules* **1997**, *30*, 2151–2158.
- (4) Borkovec, M.; Koper, G. J. M. *Prog. Colloid Polym. Sci.* **1991**, *109*, 142–152.
- (5) Koper, G. J. M.; Borkovec, M. *J. Chem. Phys.* **1996**, *11*, 4204–4213.
- (6) Smits, R. G.; Koper, G. J. M.; Mandel, M. *J. Phys. Chem.* **1993**, *97*, 5745–5751.
- (7) Borkovec, M.; Koper, G. J. M. *J. Phys. Chem.* **1994**, *98*, 6038–6045.
- (8) Kawaguchi, S.; Kitano, T.; Ito, K. *Macromolecules* **1991**, *24*, 6030–6036; *Macromolecules* **1992**, *25*, 1294–1299.
- (9) de Groot, J.; Koper, G. J. M.; Borkovec, M.; de Bleijser, J. *Macromolecules* **1998**, *31*, 4182–4188.
- (10) Reed, C. E.; Reed, W. F. *J. Chem. Phys.* **1992**, *96*, 1609–1620.
- (11) Ullner, M.; Jonsson, B. *Macromolecules* **1996**, *29*, 6645–6655.
- (12) Ullner, M.; Jonsson, B.; Soderberg, B.; Peterson, C. *J. Chem. Phys.* **1996**, *104*, 3048–3057.
- (13) Jonsson, B.; Ullner, M.; Peterson, C.; Sommelius, O.; Soderberg, B. *J. Phys. Chem. B* **1996**, *100*, 409–417.
- (14) Ullner, M.; Jonsson, B.; Widmark, P. O. *J. Chem. Phys.* **1994**, *100*, 3365–3366.
- (15) Borkovec, M. *Langmuir* **1997**, *13*, 2608–2613.
- (16) Tomalia, D. A.; Naylor, A. M.; Goddard, W. A., III. *Angew. Chem., Int. Ed. Engl.* **1990**, *29*, 138–175.
- (17) Frechet, J. M. J. *Science* **1994**, *263*, 710–714.
- (18) van Duijvenbode, R. C.; Borkovec, M.; Koper, G. J. M. *Polymer* **1998**, *39*, 2657–2664.

- (19) Koper, G. J. M.; van Genderen, M. H. P.; Elissen-Román, C.; Baars, M. W. P. L.; Meijer, E. W.; Borkovec, M. *J. Am. Chem. Soc.* **1997**, *119*, 6512–6521.
- (20) Baxter, R. J. *Exactly Solved Models in Statistical Mechanics*; Academic Press: New York, 1982.
- (21) Fikentscher, R.; Miksovsky, F. DE 1 941 175 (BASF Aktiengesellschaft), 1969.
- (22) St. Pierre, T.; Geckle, M. *J. Macrom. Sci. Chem.* **1985**, *A22*, 877–887.
- (23) Lukovkin, G. M.; Pshezhetsky, V. S.; Murtazaeva, G. A. *Eur. Polym. J.* **1973**, *9*, 559–565.
- (24) Smits, R. G. Physical Properties of Aqueous Solutions of Linear Poly(Ethyleneimine). Ph.D. Thesis, Leiden University, Leiden, The Netherlands, 1994.
- (25) Scherr, G.; Steuerle, U.; Fikentscher, R. *Kirk-Othmer's Encyclopedia of Chemical Technology*; Wiley: New York, 1995; Vol. 14, pp 2–40.
- (26) Roark, D. N.; McKusick, B. C.; Steuerle, U. *Ullmann's Encyclopedia of Industrial Chemistry*, 6th ed.; Verlag Chemie: Weinheim, Germany, 2002; in press.
- (27) Kinniburgh, D. G.; Milne, C. J.; Venema, P. *Soil Sci. Soc. Am. J.* **1995**, *59*, 417–422.
- (28) van Duijvenbode, R. C.; Rajanayagam, A.; Koper, G. J. M.; Borkovec, M.; Paulus, W.; Steuerle, U.; Häussling, L. *Phys. Chem. Chem. Phys.* **1999**, *1*, 5649–5652.

MA020819S